Star-Polymer-DNA Gels
Showing Highly Predictable and Tunable Mechanical Responses

*Masashi Ohira[1], Takuya Katashima[1], Mitsuru Naito[2], Daisuke Aoki[3], Yusuke Yoshikawa[4], Hiroki Iwase[5], Shin-ichi Takata[6], Kanjiro Miyata[7], Ung-il Chung[1], Takamasa Sakai[1], Mitsuhiro Shibayama[5] and Xiang Li[8]**

[1]*Department of Bioengineering, Graduate School of Engineering, The University of Tokyo, 7-3-1 Hongo, Bunkyo-ku, Tokyo, 113-8685, Japan*
[2]*Center for Disease Biology and Integrative Medicine, Graduate School of Medicine, The University of Tokyo, 7-3-1 Hongo, Bunkyo-ku, Tokyo, 113-0033, Japan*
[3]*Department of Chemical Science and Engineering, Tokyo Institute of Technology, 2-12-1 Ookayama, Meguro-ku, 152-8550, Tokyo, Japan*
[4]*Neutron Science Laboratory, Institute for Solid State Physics, The University of Tokyo, 5-1-5 Kashiwanoha, Kashiwa, Chiba 277-8581, Japan*
[5]*Neutron Science and Technology Center, Comprehensive Research Organization for Science and Society (CROSS), 162-1 Shirakata, Tokai, Naka, Ibaraki, 319-1106, Japan*
[6]*Materials and Life Science Division, J-PARC Center, Japan Atomic Energy Agency (JAEA), 2-4 Shirakata, Tokai, Ibaraki 319-1195, Japan*
[7]*Department of Materials Engineering, Graduate School of Engineering, The University of Tokyo, 7-3-1 Hongo, Bunkyo-ku, Tokyo, 113-8656, Japan*
[8]*Faculty of Advanced Life Science, Hokkaido University, Sapporo 001-0021, Japan*

*Correspondence to: Xiang Li, x.li@sci.hokudai.ac.jp

Keywords: self-assembly, viscoelasticity, stress relaxation, thermodynamics, kinetics

Abstract

Dynamically crosslinked gels are appealing materials for applications that require time-dependent mechanical responses. DNA duplexes are ideal crosslinkers for building such gels because of their excellent sequence addressability and flexible tunability in bond energy. However, the mechanical responses of most DNA gels are complicated and unpredictable despite the high potential of DNA. Here, we demonstrate a DNA gel with a highly homogeneous gel network and well-predictable mechanical behaviors by using a pair of star-polymer-DNA precursors with presimulated DNA sequences showing the two-state transition. The melting curve analysis of the DNA gels reveals the good correspondence between the thermodynamic potentials of the DNA crosslinkers and the presimulated values by DNA calculators. Stress-relaxation tests and dissociation kinetics measurements show that the macroscopic relaxation time of the DNA gels is approximately equal to the lifetime of the DNA crosslinkers over four orders of magnitude from 0.1-2,000 sec. Furthermore, a series of durability tests find the DNA gels are hysteresis-less and self-healable after the applications of repeated temperature and mechanical stimuli. These results demonstrate the great potential of star-polymer-DNA precursors for building gels with predictable and tunable viscoelastic properties, suitable for applications such as stress-response extracellular matrices, injectable solids, and soft robotics.

(198 words)

Introduction

Dynamically crosslinked gels provide time-dependent mechanical responses, with a stiff structure for a short time but a flowing nature over a long time[1]. The unique physical properties of these gels are attributed to the repeated breaking and reforming of the crosslinkers that bridge the polymer chains in the gels[2]. Because of the transient behavior of dynamically crosslinked gels, a variety of applications have been explored, including injectable solids[3,4], stress-response extracellular matrices[5–7], impact-resistant materials[8,9], and self-healable and recyclable materials[10–12].

Small DNA duplexes, formed by hybridizing a pair of oligo DNA with complementary sequences (**Figure 1a**), are promising crosslinkers for building dynamically crosslinked gels because oligo DNA has unique advantages of high biocompatibility, water solubility, sequence addressability, and temperature sensitivity[13–15]. In addition, studies have revealed that the bond energy of the DNA duplexes can be continuously tuned over a vast range from ~50 to ~120 kJ mol^{-1} by changing the sequences and the length of the DNA[16–18]. The continuous tunability is challenging for other dynamic crosslinkers, especially at the physiological conditions (pH 7.4, 37°C) where the temperature and pH are fixed [19–21]. Ideally, by properly designing the DNA sequences, we could deliberately fabricate dynamically crosslinked gels with any desired viscoelastic properties.

To utilize the advantages of DNA duplexes, numerous DNA hydrogels have been developed [22,23]. However, in most DNA gels, the viscoelastic properties were not ideal because the formed gel networks were highly heterogeneous and uncontrollable[24–26]. The random and complicated gel network induces untraceable mesoscopic pathways between duplex dissociation/association and the gel's mechanical responses. Despite the accumulated knowledge and databases on the thermodynamics[27,28] and kinetics[29,30] of DNA duplexes, it is challenging to fabricate DNA gels with on-demand viscoelastic properties.

Recent studies on covalently crosslinked gels have shown that network homogeneity can be substantially improved by using monodisperse star polymers as gel-forming precursors[31–34]. Several researchers have modified the end groups of star polymers with dynamic crosslinkers, such as metal-coordinate bonds[19,35,36], dynamic covalent bonds[37–41], and host-guest bonds[21,42], to prepare homogeneous dynamically crosslinked gels. These gels exhibited an

excellent one-to-one correspondence between the crosslinker lifetime and the gel stress relaxation time[37,40,41]. Although a similar strategy was employed for DNA gels, the viscoelastic properties of the DNA gels were still complicated[20,43]. Moreover, the gel network homogeneity and relation between the DNA sequences and the gel's viscoelastic properties have not yet been investigated.

In this study, to exploit the potential of DNA duplexes as dynamic crosslinkers, we fabricated well-defined star-polymer-DNA gels by hybridizing a pair of four-armed poly(ethylene glycol) (PEG) terminated with oligo DNA strands with presimulated DNA sequences. The DNA sequences were designed to undergo a simple two-state transition from duplex to single strands without forming stable intermediates. We observed repetitive sol-gel transitions by changing the temperatures and applying force to the gels. The high homogeneity of the star-polymer-DNA gel was confirmed using contrast-matched small-angle neutron scattering. We also tested the mechanical responses of the DNA gels and the dissociation kinetics of the DNA duplexes. The macroscopic stress relaxation time was perfectly consistent with the microscopic DNA duplex lifetime over a range of approximately four orders of magnitude. These results confirm for the first time the high potential of DNA duplexes as predictable and tunable crosslinkers for the preparation of dynamically crosslinked gels.

Results and Discussion

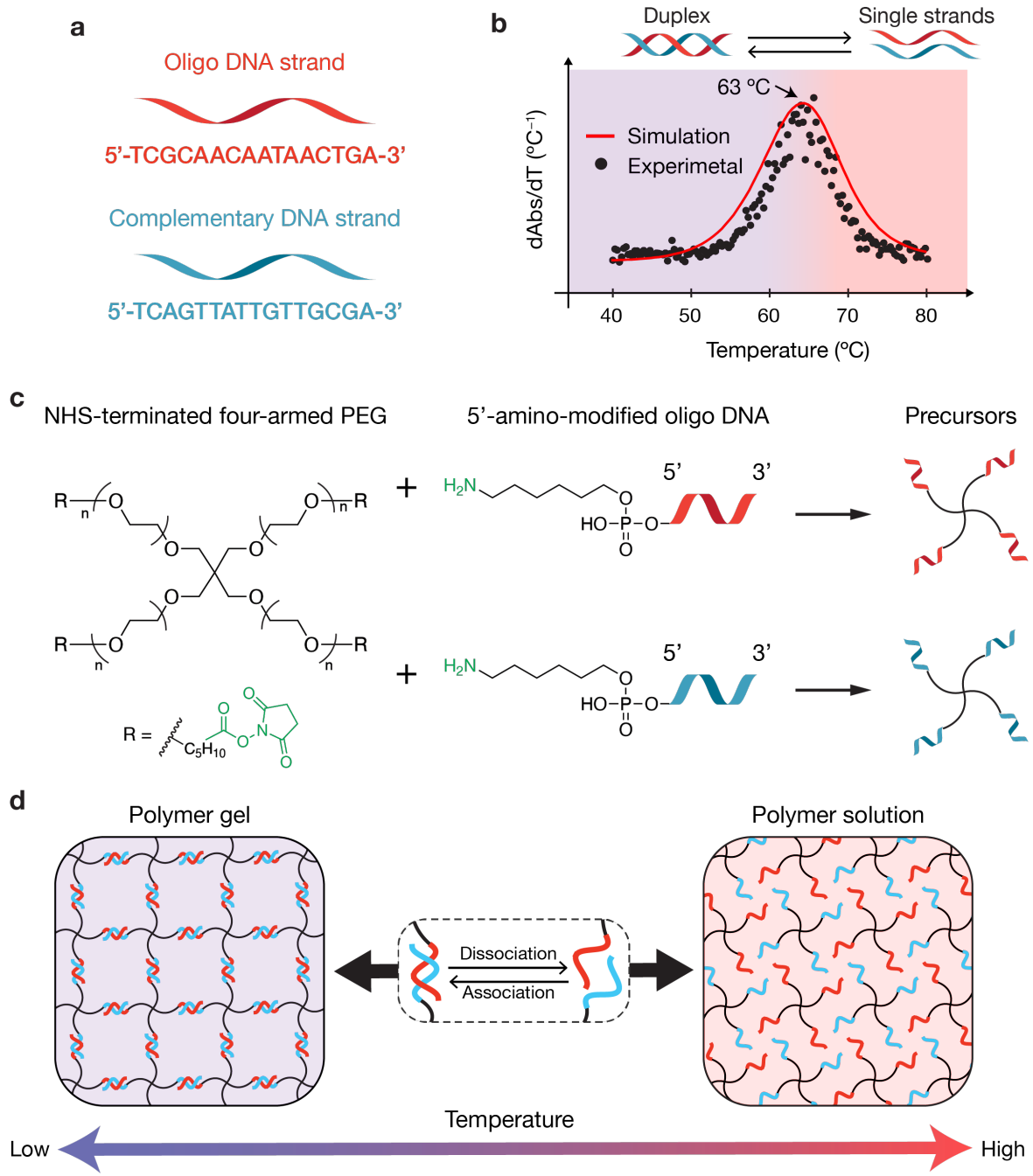

Figure 1. Schematic illustration of star-polymer-DNA gels. a, A pair of oligo DNA strands with complementary sequences designed in this study. **b**, The first derivatives of the simulated and experimentally measured melting curves (*dAbs*/*dT*) for the designed sequences. Here, *Abs* is the absorbance of UV light (260 nm) in the DNA solution, and *T* is the temperature. **c**, Synthesis scheme of the two types of four-armed gel-forming precursors terminated with oligo DNA strands with complementary sequences. **d**, An illustration of a star-polymer-DNA gel

that exists in gel form at low temperatures and becomes a solution at high temperatures, corresponding to the association and dissociation of the DNA duplexes.

Using an online oligo DNA simulator, DINAMelt[44] and NUPACK[45], we designed a pair of small complementary DNA sequences (16 mer) (**Figure 1a, Figures S1 and S2**). The simulated quasistatic dissociation curves of the oligo DNA showed a simple two-state transition from duplexes to single strands as the temperature was raised; the formation of nonideal associations, e.g., stem-loops, was negligible in the simulated results (**Figures S1 and S2**). We evaluated the real dissociation curve of the DNA duplex by measuring the UV absorbance of the DNA solution at different temperatures, i.e., melting curve analysis (**Figure 1b**). To remove the irrelevant linear changes in the absorption coefficients of the DNA strands, we took the first derivative of the experimental melting curve and compared it with the simulated curve. The real dissociation curve agreed well with the simulated curve, confirming the high accuracy of the established DNA thermodynamics database in predicting real behavior. The temperature at which 50% of the DNA duplexes dissociated, i.e., the melting temperature, was set to approximately 63°C for this study to ensure the stability of the DNA duplexes under physiological conditions (~37°C, pH 7.4). The melting temperature could be flexibly tuned over a range from ~5°C to ~90°C by changing the sequences and length of the oligo DNA[46,47].

After confirming the performance of the oligo DNA, we conjugated these oligo strands to four-armed poly(ethylene glycol) (4arm-PEG, M_n = 40 kg mol^{-1}) to prepare two types of star-polymer-DNA precursors with complementary sequences (**Figure 1c**). The four-arm PEG was terminated with an active ester group (NHS ester) at each arm end, and the oligo DNA was terminated with a primary amine at the 5' terminal. Conjugation of DNA and four-armed PEG was performed by using the NHS-ester/amine reaction. The conjugation ratio of the oligo DNA strand per PEG arm was as high as 95%, as determined with reversed-phase chromatography (**Figures S3 and S4, Table S1**). The mixed solution with two star-polymer-DNA precursors is expected to remain in the liquid phase at high temperatures and form a gel at low temperatures, corresponding to the dissociation of DNA duplexes and the association of DNA strands, respectively (**Figure 1d**).

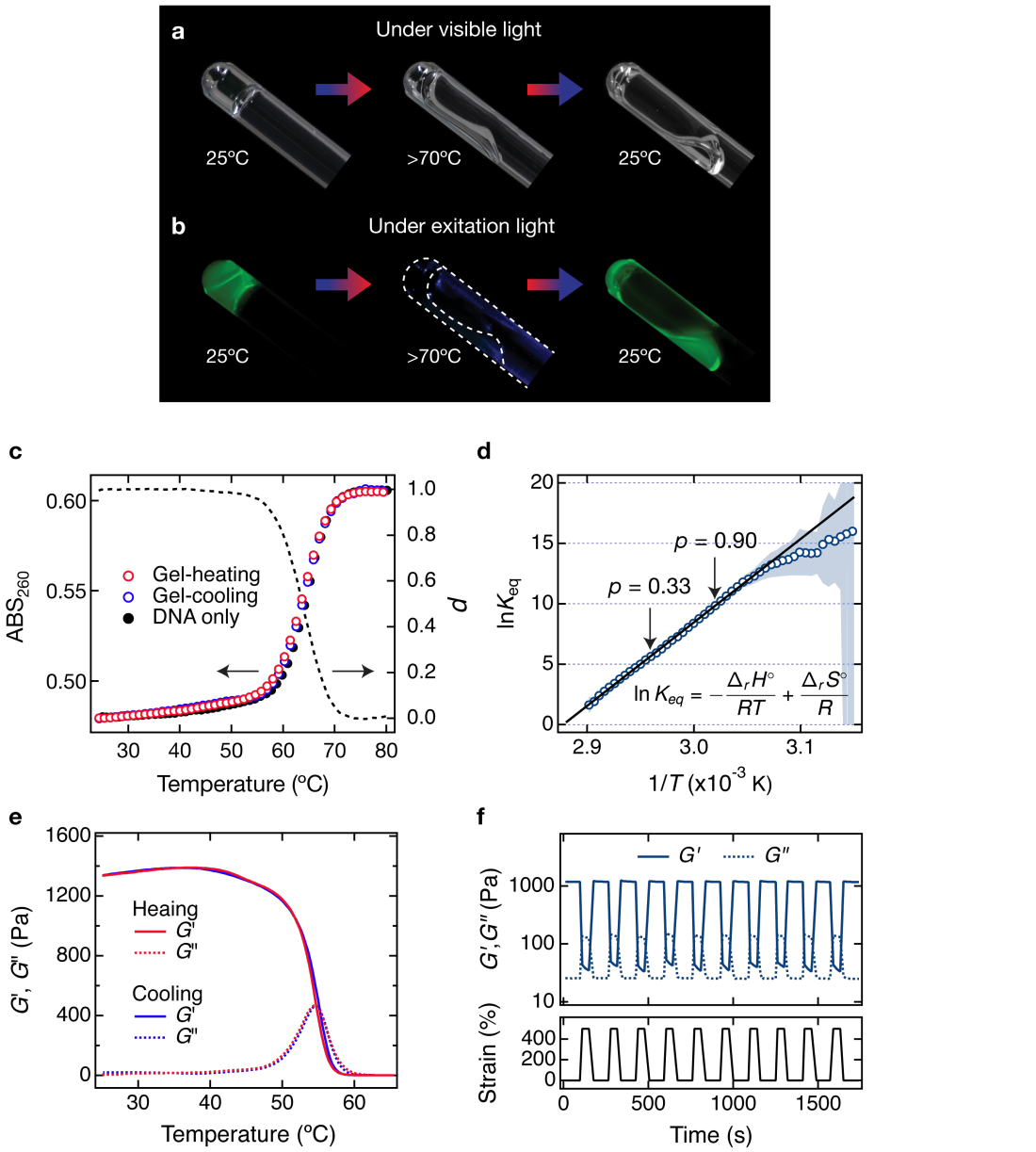

Figure 2. Sol-gel transition of DNA hydrogels. a, Photographs of the DNA hydrogel showing repetitive sol-gel transitions in a glass tube at different temperatures. **b**, Corresponding fluorescence images of the DNA hydrogel. A duplex-sensitive fluorescence dye, which emits green fluorescent light in the presence of DNA duplexes, was added to the gel. **c**, Melting curves of the DNA hydrogel during heating and cooling processes. A solution with only DNA duplexes with the same DNA concentration as in the gel was used as a control; the melting curve of the DNA-only solution was vertically scaled by a factor of 1.078 to correct the slight difference in the DNA concentration. The crosslinking degree (p), i.e., the hybridization degree of the DNA, was calculated from the gel's melting curve by assuming a two-state transition model. **d**, Temperature dependence of the equilibrium constant (K_{eq}) for DNA duplex dissociation. The solid line shows the fit result with the van't Hoff equation. **e**, Mechanical

properties of the DNA gel during heating and cooling measured at an oscillation frequency of 1 Hz. **f**, Self-healing of the DNA hydrogel confirmed by a repetitive strain recovery test.

We dissolved the two types of precursors in sodium phosphate buffer solutions (pH 7.4, 25 mM), respectively, at a precursor concentration of 1 mM. The two precursor solutions were mixed in a test tube immersed in a hot water bath and then cooled to ambient temperature; a transparent hydrogel was formed immediately (**Figure 2a**). The gel showed repetitive sol-gel transitions upon heating and cooling the gel above and below the melting temperature of the DNA duplex (~63°C). The formation and dissociation of the DNA duplex in the gel were confirmed by adding a small amount of a duplex-sensitive fluorescent dye, SYBR Green I, into the gels (**Figure 2b**). Green fluorescence was observed in the gel and disappeared in the sol, indicating that duplex formation induced gelation.

Quantitative analysis of the crosslinking extent was performed by measuring the gels' melting curves. After heating the gels, the UV absorbance started to increase at 55°C and reached a plateau at 75°C, indicating the dissociation of DNA duplexes at high temperatures (**Figure 2c**). The same UV absorbance curve was observed in the backward process from high to low temperatures; no hysteresis was observed for the DNA duplex formation and dissociation processes in the gels. In addition, the gel melting curves were consistent with that of a DNA-only solution at the same concentration (**Figure 2c**, filled black circles), suggesting that the thermodynamic behavior of the oligo DNA was not disturbed by gel network formation.

The crosslinking ratio (p) between the precursors, i.e., the fraction of the DNA duplexes in the gel, was estimated from the gel melting curves (**Figure 2c, Figure S5, Table S2**). According to Flory-Stockmayer theory[48], the gelation point for covalently crosslinked gels is at $p = 1/3$, which is approximately equal to 65°C for our DNA gel. However, we need to note that there is no clear gelation point for dynamically crosslinked gels because the gelation points of these gels depend on the observation time scale, similar to glasses. Therefore, we converted p to a more indicatory parameter, namely, the equilibrium constant of DNA hybridization (K_{eq}). K_{eq} can be written as a function of p as $K_{eq} = 2pc^{o}/((1-p)^2C_T)$ by assuming the two-state transition model (**SI Section 4.1**). Here, c^{o} is a standard molar concentration whose value is typically 1 mol L^{-1}, and C_T is the total molar concentration of DNA strands. A linear van't Hoff temperature dependence was confirmed between the equilibrium constant and the temperature

(**Figure 2d**). We estimated the thermodynamic potentials by fitting the equilibrium constants using the van't Hoff equation, $\ln K_{eq} = -(\Delta_r H^o)/RT + (\Delta_r S^o)/R$, where $\Delta_r H^o$ and $\Delta_r S^o$ are the standard enthalpy and standard entropy for the duplex formation and R is the gas constant. $\Delta_r H^o$ and $\Delta_r S^o$ were estimated to be −577 kJ mol^{-1} and –1.58 kJ mol^{-1} K^{-1}, respectively. The $\Delta_r H^o$ value for network formation in the star-polymer-DNA gel was approximately ten times higher than that of the other dynamically crosslinked gels (e.g., −68 kJ mol^{-1} for diarylbibenzofuranone[49]; −60 kJ mol^{-1} for the reversible Diels-Alder reaction[35]). The unconventionally large $\Delta_r H^o$ for the star-polymer-DNA gels was attributed to the unique base stacking effect of the DNA[50]. The large $\Delta_r H^o$ of the DNA also suggests that the thermodynamic stability of star-polymer-DNA gels can be vastly tuned by a small temperature change. Gels with such high-temperature sensitivity may serve as promising materials for sensing and injectable applications. In addition, the measured standard thermodynamic potentials are in good agreement with the presimulated values of the DNA oligo calculator (**Table S2**), suggesting that we can design gels with predefined thermodynamic stability based on the calculation.

Next, we evaluated the macroscopic hysteresis and primary mechanical properties of the star-polymer-DNA gels with dynamic viscoelastic tests. The storage modulus (G') and loss modulus (G''), which are indicators of the solid and liquid responses, respectively, were measured at different temperatures at a constant oscillation frequency of 1 Hz (**Figure 2e**). G' was approximately 1300 Pa, which is much higher than G'', at ambient temperature. Upon increasing the temperature, G' decreased and fell below G'' at 55°C. G' changed by more than 100-fold with a difference of only 5°C near this crossover point, which was attributed to the large $\Delta_r S^o$ of the DNA duplex, as observed from the melting curve analysis. The same G' and G'' curves were observed during the cooling process. We repeated the heating and cooling procedures at least six times but did not observe any hysteresis in the mechanical properties (**Figure S6**).

We also observed instant self-healing of the gel via break and recovery experiments (**Figure 2f**). When a large oscillatory strain (~ 500%) was applied to the gel, G' decreased from 1300 Pa to 20 Pa, and the gel completely broke. In contrast, after removing the large strain, G' immediately recovered to the original value. The same break and recovery tests were repeated for at least ten cycles, and the recovery ratio of G' was almost 100%. The perfect recovery of G' indicates that the breakage of the gel occurred selectively at the crosslinkers, i.e., the DNA

duplexes, but not within the main PEG network. Thermodynamically stable but moderately weak properties suggest the high potential of DNA duplexes as dynamic crosslinkers.

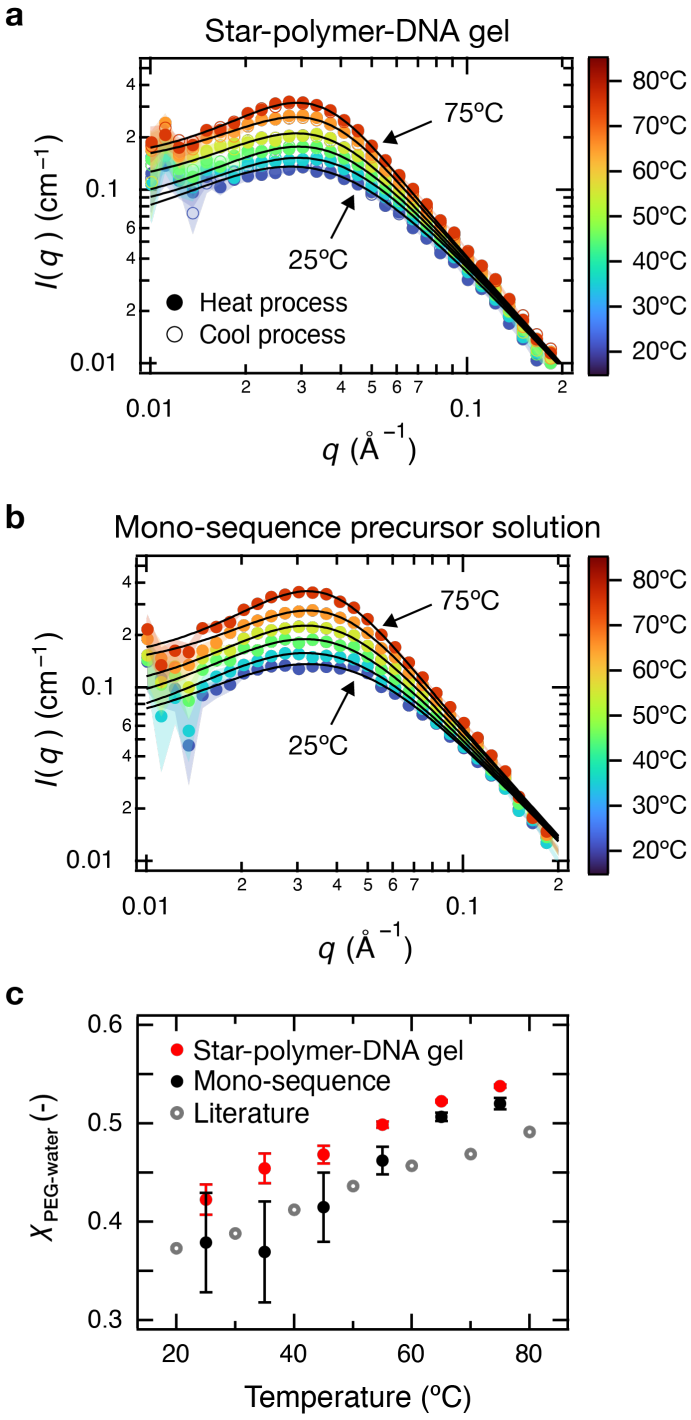

Figure 3. Network structures of star-polymer-DNA gels at different temperatures measured via small-angle neutron scattering (SANS). a, Scattering profiles ($I(q)$) of the star-polymer-DNA gel during heating and cooling. Here, q is the magnitude of the scattering vector. Since the solvent contrast was matched to that of the DNA, the correlation between

four-armed PEG, which is located at the center of the precursors, was exclusively observed. The solid curves denote the fit results using a model scattering function for four-armed star block copolymers (**SI Section 4.2**). **b**, Scattering profile of a monosequence solution; this solution does not form a gel at any temperature. The solvent contrast was matched to that of the DNA as well as the gel sample. The solid curves denote the fit results using the same model function used in the gel's scattering profiles. **c**, Energy interaction parameters between PEG and water ($\chi_{\text{PEG-water}}$) at different temperatures. The $\chi_{\text{PEG-water}}$ values were obtained from the model function fits (**SI Section 4.2**). The literature values for a PEG/pure water system are displayed for comparison[51].

The nanostructure of the star-polymer-DNA hydrogels was evaluated with small-angle neutron scattering (SANS). We matched the scattering contrast of the solvent to that of the DNA strands by tuning the H_2O/D_2O ratio in the buffer solution (**Figure S7**). Under this contrast-matched condition, the scattering from the DNA strands was masked, and we exclusively observed correlations from the PEG polymers, i.e., the central region of the precursors. **Figure 3a** shows the scattering intensity $I(q)$ as a function of the magnitude of the scattering vector, q. A broad peak was observed at $q \sim 0.03$ Å^{-1}, denoting the correlation of the PEG polymers. The peak height increased as the temperature was raised, but the peak position remained unchanged. The constant peak position indicates that the PEG polymers in the precursors were separated from each other at a constant distance independent of the crosslinking ratio, suggesting that the gel network of the star-polymer-DNA gel is highly homogeneous.

To understand the change in the peak height, we analyzed a precursor solution with only one type of sequence, which does not form a gel at any temperature. The scattering profiles of the monosequence precursor solution were identical to those of the gel at all temperatures (**Figure 3b**). The good consistency between the profiles of the star-polymer-DNA gel and the monosequence precursor solution confirms that no heterogeneous structures were formed during the gelation. In addition, the same temperature dependence between the gel and the monosequence profiles suggest that the change in the peak height was irrelevant to the sol-gel transition. By fitting the scattering profiles with a model function for star block copolymers under contrast-matched conditions[52] (**Figure 3a, b and SI Section 4.2**), we found that the difference in the peak height was attributed to the changes in the energy interaction between the PEG polymers and the water molecules at different temperatures. The estimated energy

interaction parameters (χ) were displayed as a function of temperature (**Figure 3c**, **Figure S8**). The interaction parameters between PEG and water $\chi_{PEG\text{-}water}$ are close to the reference values of PEG measured in pure water[51]. When the energy interaction parameter between a polymer and a solvent is above 0.5, the polymer tends to form aggregates. However, such aggregation was not observed in our star-polymer-DNA gel. The negatively charged DNA strands terminated at the ends of four-armed PEG may have enhanced the solubility of PEG at high temperatures, which could be confirmed by the turbidity tests (**Figure S9**). The excellent stability of the star-polymer-DNA precursors may be a reason for the extremely low hysteresis and instant self-healing behavior observed in **Figure 2**.

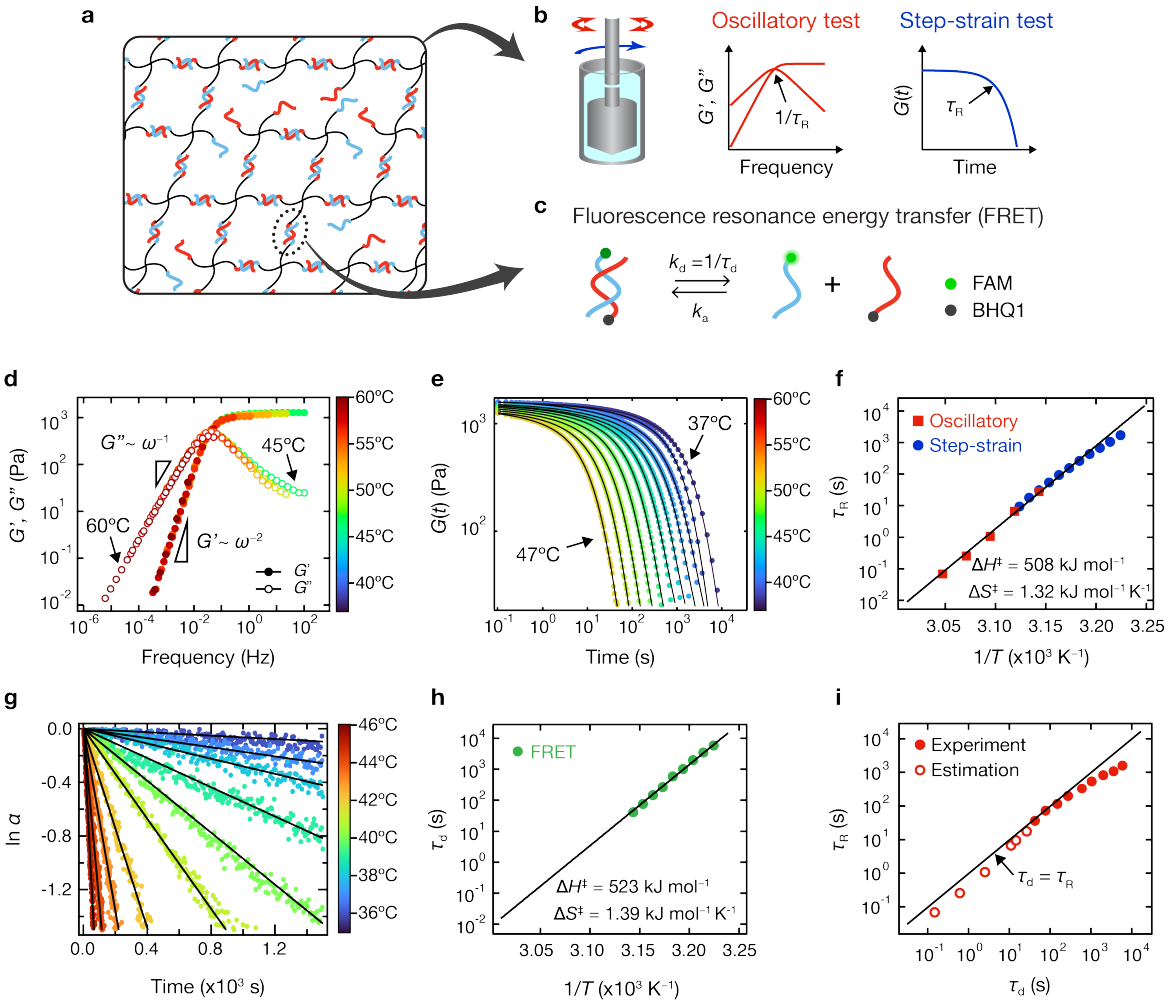

Figure 4. Relationship between gel stress relaxation and DNA duplex dissociation. a, An illustration of the deformed star-polymer-DNA network. **b,** The viscoelastic properties of the gels were characterized with a rheometer using two different methods: an oscillatory test for fast relaxation at high temperatures and a step-strain test for slow relaxation at low

temperatures. **c,** The duplex dissociation kinetics were evaluated for DNA-only solutions using fluorescence resonance energy transfer (FRET). **d**, Master curves of G' and G'' obtained from the oscillatory test for star-polymer-DNA gels over the range of 45-60°C at intervals of 2.5°C. The master curves were prepared by the time-temperature superposition treatment, using the curves at 45°C as reference **e**, Stress relaxation curves of star-polymer-DNA gel obtained from the step-strain tests over the range of 37-47°C at 1°C intervals. **f**, Temperature dependence of the stress relaxation time of the gels (τ_R). **g**, Time variation of the normalized molar concentration of DNA duplexes (α) obtained from FRET measurements over the temperature range of 36-45°C at 1ºC intervals. **h**, Temperature dependence of the lifetime of the DNA duplexes (τ_d). **i**, Correlation plot of τ_R with respect to τ_d. The τ_d values in the experimentally inaccessible time range were estimated using the Eyring equation and displayed as open circles to distinguish them from the experimentally measured τ_d values (filled circles). All τ_R values were obtained experimentally. The solid line denotes a guide for the one-to-one correspondence limit ($\tau_R = \tau_d$), where the macroscopic stress relaxation is directly linked with the microscopic dissociation of the DNA duplexes.

Finally, we evaluated the detailed linear mechanical responses of the star-polymer-DNA gels (**Figure 4a**). We used two different methods to cover a wide test time range: oscillatory tests and step-strain tests (**Figure 4b**). The linear viscoelastic region was assessed using the strain sweep tests (**Figure S10**). The corresponding microscopic dissociation kinetics of the DNA duplexes were monitored separately using a fluorescence resonance energy transfer (FRET) technique (**Figure 4c**).

For quick responses relaxing within 10 seconds, the mechanical parameters G' and G'' were measured via oscillatory tests as a function of the oscillation frequency (ω). The master curves were constructed by horizontally scaling G' and G'' at different temperatures on the basis of time-temperature superposition treatment using 45°C as a reference temperature (**Figure 4d**). The scaled curves overlapped well with each other and could be represented by a single Maxwell element[53], where $G' \sim \omega^2$ and $G'' \sim \omega^1$ at low frequencies and $G' \sim \omega^0$ and $G'' \sim \omega^{-1}$ at high frequencies (**SI Section 4.3**). Such simple viscoelastic behavior was not observed in the randomly crosslinked DNA gels[26] and the DNA gels with sequences not showing the two-state transition[20,43]. The high homogeneity of the star-polymer-DNA gel and its well-designed DNA sequences showing the two-state transition likely simplified the relaxation behavior of

the DNA gels. A characteristic stress relaxation time, which corresponds to the cross point of the G' and G" curves, was more precisely estimated by fitting each curve with the Maxwell model (**Figure S11**) and is shown later.

On the other hand, for mechanical responses relaxing in more than 10 seconds, we used step-strain tests. After applying the step strain on the gels, the stress ($G(t)$) on the gels gradually decayed as the gel network relaxed (**Figure 4e**). The stress relaxation time of the star-polymer-DNA gels changed by more than two orders of magnitude with a temperature difference of 10°C. Such a strong temperature dependence of the viscoelastic properties has never been reported in other dynamically crosslinked gels. We precisely estimated the characteristic relaxation time by fitting the slowest relaxation mode in each curve (**SI Section 4.4**). The relaxation times obtained from the above two mechanical measurements were plotted as a function of $1/T$ (**Figure 4f**). The obtained values fell on a single straight line and partially overlapped at intermediate temperatures. We analyzed the temperature dependence of τ_R using the Eyring equation, $1/\tau = (k_B T/h)\exp(-\Delta H^{\ddagger}/RT+\Delta S^{\ddagger}/R)$, where k_B is the Boltzmann constant, h is the Planck constant, $\Delta H^{\ddagger}$ and $\Delta S^{\ddagger}$ are the activation enthalpy and entropy of duplex dissociation. The $\Delta H^{\ddagger}$ and $\Delta S^{\ddagger}$ are estimated to be 508 kJ mol^{-1} and 1.32 kJ mol^{-1} K^{-1}. The $\Delta H^{\ddagger}$ value for the DNA duplex dissociation is much higher than the $\Delta H^{\ddagger}$ of the other dynamically crosslinked polymer materials: 30-90 kJ mol^{-1} for host-guest bonds[54], 47-85 kJ mol^{-1} for the phenanthroline-metal complex[55], 64 kJ mol^{-1} for oxime−ester bonds[56], and 111 kJ mol^{-1} for urethane bonds[57].The result accounts for the temperature-sensitive stress relaxation behavior of the star-polymer-DNA gels. The abnormally large $\Delta H^{\ddagger}$ for the DNA duplex dissociation is due to the stable double-helix structures of DNA, enhanced by the base stacking effect and multiple hydrogen bonds between the bases[50].

After determining the macroscopic relaxation time of the gels, we measured the lifetime of the DNA duplexes (τ_d), which is equal to the reciprocal of the duplex dissociation rate constant ($\tau_d = 1/k_d$). Because the association and dissociation processes are in equilibrium in the gels, it is difficult to measure each rate constant separately. Therefore, we deliberately created nonequilibrium conditions by dropping a small volume of concentrated DNA duplex solution into a large buffer solution. For a short time, the dissociation of the DNA duplexes is the primary process, and we can exclusively evaluate the dissociation kinetics. We used the FRET technique to monitor the time variation in the number of single-stranded DNA molecules. We modified the 3'-ends of the oligo DNA and the complementary DNA with fluorescein (FAM)

and black hole quencher 1 (BHQ1), respectively (**Figure 4c**). When the DNA strands form a duplex, the quencher is in proximity to the fluorophore and suppresses its fluorescence. On the other hand, when the duplexes dissociate, the quenchers diffuse away from the fluorophore; therefore, we observed an increase of fluorescence as a signal of duplex dissociation. We confirmed that modification of the 3'-ends did not influence the thermodynamic parameters of DNA duplex formation (**Figure S12, SI Section 4.5**).

We converted the measured fluorescence intensities to the normalized molar concentrations of the duplex DNA (α), rescaled by the initial duplex concentration (**Figure 4g**, **SI Section 4.6**). The dissociation rate constant (k_d) was estimated from the initial slope in **Figure 4g** by assuming that the dissociation of the DNA duplexes was a first-order reaction over a short time (**SI Section 4.6**). The obtained k_d was converted to the lifetime ($\tau_d = 1/k_d$) of the DNA duplex and analyzed using the Eyring equation (**Figure 4h**). The estimated $\Delta H^{\ddagger}$ and $\Delta S^{\ddagger}$ for the duplex dissociation are the almost same as activation potentials for the macroscopic gel stress relaxation, suggesting that the dissociation of the DNA duplexes was the primary process inducing the relaxation of the gel networks. The direct transmission from the microscopic bond breaking to the macroscopic network relaxation was attributed to the homogeneous gel networks formed by the star-polymer-DNA precursors and the simple two-state transition of the well-designed DNA sequences.

To visualize the excellent correspondence between the macroscopic stress relaxation and the microscopic duplex dissociation in the star-polymer-DNA gels, we constructed a correlation plot for τ_R and τ_d (**Figure 4i**),. Due to the experimental limitations associated with the FRET measurements, the accessible duplex dissociation time was limited to times longer than 30 seconds. Therefore, we estimated the inaccessible τ_d values at the temperatures where the mechanical tests were performed, using the Eyring equation and the aforementioned $\Delta H^{\ddagger}$ and $\Delta S^{\ddagger}$ values. The correlation plots with the theoretically estimated τ_d values are displayed as open circles to distinguish them from those with the experimentally measured τ_d values (filled circles) (**Figure 4i**). The τ_R and τ_d values of the star-polymer gels are strongly correlated, close to the guideline for the one-to-one correspondence limit ($\tau_R = \tau_d$) over a range of nearly four orders of magnitude in time from 0.1 second to 2,000 seconds (**Figure 4i**). Such a wide correspondence between the micro- and macrorelaxation times has not been reported for any other gels. In addition, the relaxation time of the star-polymer-DNA gels under physiological conditions (37°C, pH 7.4) was approximately 2,000 seconds, which is close to the relaxation

time of tissues in the body (~ 1,000 seconds)[5,7]. This result is in stark contrast to the dynamically crosslinked star polymer gels with the other crosslinkers, which typically undergo relaxation within a minute under physiological conditions (**Figure S15**, **Supporting Spreadsheet**).

Conclusion

This work demonstrated a homogeneous DNA gel with highly predictable mechanical behaviors. We used a recently-proved star polymer strategy to improve the homogeneity of the gel network and designed a pair of DNA sequences showing a two-state transition as the dynamic crosslinkers. The formed gels responded to multiple stimuli, such as temperature and forces, and were still self-healable and hysteresis-less. The contrast-matched SANS measurements confirmed the high spatial homogeneity of the gel network. UV spectroscopy determined that the two-state transition of the DNA duplexes occurred in the gels, the same as the simulated results from the DNA calculator. In addition, stress-relaxation tests and dissociation kinetics measurements revealed that the macroscopic relaxation time of our DNA gels agreed with the lifetime of the DNA crosslinkers over an extended time range from 0.1-2,000 sec, which was not achieved by any other DNA gels. In combination with the demonstrated star-polymer-DNA gel scheme with the well-established database for DNA thermodynamics and kinetics, we will be able to fabricate DNA gels with on-demand viscoelastic properties. We envision that highly predictable and tunable star-polymer-DNA gels can boost the fundamental understanding and applications of dynamically crosslinked gels.

Supporting Information

Supporting Information is available.

Acknowledgments

This study was supported by Japan Society for the Promotion of Science (JSPS) KAKENHI grants to X.L. (JP17K14536, JP19K15628), M.O. (JP20J22044), T.K. (JP20K15338), and M.S. (JP16H02277). This study was also supported by Japan Science and Technology Agency (JST)

grants to X.L. (FOREST Program JPMJFR201Z), T.K. (COI Grant Number JPMJCE1304), M.N. (COI Grant Number JPMJCE1305), and T.S. (CREST JPMJCR1992). The SANS experiments were performed at the Materials and Life Science Experimental Facility (MLF; BL15 TAIKAN), Japan Proton Accelerator Research Complex (J-PARC), Ibaraki, Japan (Proposal no. 2017B0138).

References

[1] C. J. Kloxin, C. N. Bowman, *Chem Soc Rev* 2013, *42*, 7161.

[2] A. M. Rosales, K. S. Anseth, *Nat Rev Mater* 2016, *1*, 287.

[3] C. Loebel, C. B. Rodell, M. H. Chen, J. A. Burdick, *Nat Protoc* 2017, *12*, 1521.

[4] L. M. Stapleton, A. N. Steele, H. Wang, H. L. Hernandez, A. C. Yu, M. J. Paulsen, A. A. A. Smith, G. A. Roth, A. D. Thakore, H. J. Lucian, K. P. Totherow, S. W. Baker, Y. Tada, J. M. Farry, A. Eskandari, C. E. Hironaka, K. J. Jaatinen, K. M. Williams, H. Bergamasco, C. Marschel, B. Chadwick, F. Grady, M. Ma, E. A. Appel, Y. J. Woo, *Nat Biomed Eng* 2019, *3*, 611.

[5] O. Chaudhuri, J. Cooper-White, P. A. Janmey, D. J. Mooney, V. B. Shenoy, *Nature* 2020, *584*, 535.

[6] C. Loebel, R. L. Mauck, J. A. Burdick, *Nat Mater* 2019, *18*, 883.

[7] O. Chaudhuri, L. Gu, D. Klumpers, M. Darnell, S. A. Bencherif, J. C. Weaver, N. Huebsch, H. Lee, E. Lippens, G. N. Duda, D. J. Mooney, *Nat Mater* 2015, *15*, 326.

[8] J.-Y. Sun, X. Zhao, W. R. K. Illeperuma, O. Chaudhuri, K. H. Oh, D. J. Mooney, J. J. Vlassak, Z. Suo, *Nature* 2012, *489*, 133.

[9] T. L. Sun, T. Kurokawa, S. Kuroda, A. B. Ihsan, T. Akasaki, K. Sato, Md. A. Haque, T. Nakajima, J. P. Gong, *Nat Mater* 2013, *12*, 932.

[10] D. L. Taylor, M. in het Panhuis, *Adv Mater* 2016, *28*, 9060.

[11] S. Wang, M. W. Urban, *Nat Rev Mater* 2020, *5*, 562.

[12] Y. Cao, Y. J. Tan, S. Li, W. W. Lee, H. Guo, Y. Cai, C. Wang, B. C.-K. Tee, *Nat Electron* 2019, *2*, 75.

[13] J. Bath, A. J. Turberfield, *Nat Nanotechnol* 2007, *2*, 275.

[14] N. C. Seeman, H. F. Sleiman, *Nat Rev Mater* 2017, *3*, 17068.

[15] M. Madsen, K. V. Gothelf, *Chem Rev* 2019, *119*, 6384.

[16] K. Bielec, K. Sozanski, M. Seynen, Z. Dziekan, P. R. ten Wolde, R. Holyst, *Physical Chemistry Chemical Physics* 2019, *21*, 10798.

[17] R. J. Menssen, A. Tokmakoff, *J Phys Chem B* 2019, *123*, 756.

[18] C. F. Guerra, F. M. Bickelhaupt, J. G. Snijders, E. J. Baerends, *J Am Chem Soc* 2000, *122*, 4117.

[19] S. C. Grindy, R. Learsch, D. Mozhdehi, J. Cheng, D. G. Barrett, Z. Guan, P. B. Messersmith, N. Holten-Andersen, *Nat Mater* 2015, *14*, 1210.

[20] G. Creusen, C. O. Akintayo, K. Schumann, A. Walther, *J Am Chem Soc* 2020, *142*, 16610.

[21] H. Chen, J. Zhang, W. Yu, Y. Cao, Z. Cao, Y. Tan, *Angewandte Chemie Int Ed* 2021, *60*, 22332.

[22] S. H. Um, J. B. Lee, N. Park, S. Y. Kwon, C. C. Umbach, D. Luo, *Nat Mater* 2006, *5*, 797.

[23] Y. Shao, H. Jia, T. Cao, D. Liu, *Accounts Chem Res* 2017, *50*, 659.

[24] W. Guo, C. Lu, R. Orbach, F. Wang, X. Qi, A. Cecconello, D. Seliktar, I. Willner, *Adv Mater* 2015, *27*, 73.

[25] S. Tanaka, K. Wakabayashi, K. Fukushima, S. Yukami, R. Maezawa, Y. Takeda, K. Tatsumi, Y. Ohya, A. Kuzuya, *Chem Asian J* 2017, *12*, 2388.

[26] C. Du, R. J. Hill, *Macromolecules* 2019, *52*, 6683.

[27] J. SantaLucia, *Proc National Acad Sci* 1998, *95*, 1460.

[28] S. Nakano, M. Fujimoto, H. Hara, N. Sugimoto, *Nucleic Acids Res* 1999, *27*, 2957.

[29] T. E. Ouldridge, P. Šulc, F. Romano, J. P. K. Doye, A. A. Louis, *Nucleic Acids Research* 2013, *41*, 8886.

[30] J. X. Zhang, J. Z. Fang, W. Duan, L. R. Wu, A. W. Zhang, N. Dalchau, B. Yordanov, R. Petersen, A. Phillips, D. Y. Zhang, *Nat Chem* 2018, *10*, 91.

[31] T. Sakai, T. Matsunaga, Y. Yamamoto, C. Ito, R. Yoshida, S. Suzuki, N. Sasaki, M. Shibayama, U. Chung, *Macromolecules* 2008, *41*, 5379.

[32] T. Matsunaga, T. Sakai, Y. Akagi, U. Chung, M. Shibayama, *Macromolecules* 2009, *42*, 1344.

[33] X. Li, S. Nakagawa, Y. Tsuji, N. Watanabe, M. Shibayama, *Sci Adv* 2019, *5*, eaax8647.

[34] X. Huang, S. Nakagawa, X. Li, M. Shibayama, N. Yoshie, *Angewandte Chemie Int Ed* 2020, *59*, 9646.

[35] D. E. Fullenkamp, L. He, D. G. Barrett, W. R. Burghardt, P. B. Messersmith, *Macromolecules* 2013, *46*, 1167.

[36] T. Rossow, A. Habicht, S. Seiffert, *Macromolecules* 2014, *47*, 6473.

[37] R. J. Sheridan, C. N. Bowman, *Macromolecules* 2012, *45*, 7634.

[38] V. Yesilyurt, A. M. Ayoob, E. A. Appel, J. T. Borenstein, R. Langer, D. G. Anderson, *Adv Mater* 2017, *29*, 1605947.

[39] G. A. Parada, X. Zhao, *Soft Matter* 2018, *14*, 5186.

[40] B. Marco-Dufort, R. Iten, M. W. Tibbitt, *J Am Chem Soc* 2020, *142*, 15371.

[41] T. M. FitzSimons, F. Oentoro, T. V. Shanbhag, E. V. Anslyn, A. M. Rosales, *Macromolecules* 2020, *53*, 3738.

[42] H. Li, Z. Duan, Y. Yang, F. Xu, M. Chen, T. Liang, Y. Bai, R. Li, *Macromolecules* 2020, *53*, 4255.

[43] C. O. Akintayo, G. Creusen, P. Straub, A. Walther, *Macromolecules* 2021, *54*, 7125.

[44] N. R. Markham, M. Zuker, *Nucleic Acids Res* 2005, *33*, W577.

[45] J. N. Zadeh, C. D. Steenberg, J. S. Bois, B. R. Wolfe, M. B. Pierce, A. R. Khan, R. M. Dirks, N. A. Pierce, *J Comput Chem* 2011, *32*, 170.

[46] J. SantaLucia, H. T. Allawi, P. A. Seneviratne, *Biochemistry-us* 1996, *35*, 3555.

[47] N. Sugimoto, S. Nakano, M. Yoneyama, K. Honda, *Nucleic Acids Res* 1996, *24*, 4501.

[48] D. R. Miller, C. W. Macosko, *Macromolecules* 1976, *9*, 206.

[49] K. Imato, A. Takahara, H. Otsuka, *Macromolecules* 2015, *48*, 5632.

[50] P. Yakovchuk, E. Protozanova, M. D. Frank-Kamenetskii, *Nucleic Acids Res* 2006, *34*, 564.

[51] J. S. Pedersen, C. Sommer, Springer Berlin Heidelberg, 2005, pp. 70–78.

[52] M. Ohira, Y. Tsuji, N. Watanabe, K. Morishima, E. P. Gilbert, X. Li, M. Shibayama, *Macromolecules* 2020, *53*, 4047.

[53] M. Rubinstein, R. H. Colby, *Polymer Physics*, Oxford University Press New York, 2003.

[54] E. A. Appel, R. A. Forster, A. Koutsioubas, C. Toprakcioglu, O. A. Scherman, *Angewandte Chemie Int Ed* 2014, *53*, 10038.

[55] T. Rossow, S. Seiffert, *Polym. Chem.* 2014, *5*, 3018.

[56] C. He, S. Shi, D. Wang, B. A. Helms, T. P. Russell, *J Am Chem Soc* 2019, *141*, 13753.

[57] D. J. Fortman, J. P. Brutman, C. J. Cramer, M. A. Hillmyer, W. R. Dichtel, *J Am Chem Soc* 2015, *137*, 14019.

Table of Contents

Star-Polymer-DNA Gels
Showing Highly Predictable and Tunable Mechanical Responses

*Masashi Ohira[1], Takuya Katashima[1], Mitsuru Naito[2], Daisuke Aoki[3], Yusuke Yoshikawa[4], Hiroki Iwase[5], Shin-ichi Takata[6], Kanjiro Miyata[7], Ung-il Chung[1], Takamasa Sakai[1], Mitsuhiro Shibayama[5] and Xiang Li[8]**

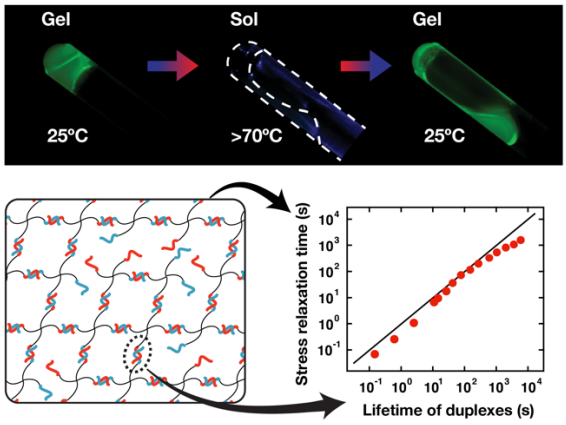

DNA gels with predictable mechanical responses are developed using a star polymer strategy and a pair of presimulated DNA sequences. The macroscopic stress relaxation time of the DNA gel is connected directly to the microscopic lifetime of the DNA crosslinkers over an extended time range from 0.1-2000 sec. In addition, the DNA gels are spatially homogeneous, hysteresis-less, and self-healable.
(59 words)